Journal of the Korean Physical Society, Vol. 49, No. 4, October 2006, pp. 1470∼1476

Measurement of the Plasma Potential in the Edge Plasma of the ORNL CAPRICE ECR Ion Source

Hyun Jong YOU* and Kyu Sun CHUNG
Department of Nuclear Engineering, Hanyang University, Seoul 133-791

Fred Wolfgang MEYER
Physics Division, Oak Ridge National Laboratory, Oak Ridge, TN 37919-6372, U.S.A.

(Received 6 July 2006)

Measurements of the plasma potential by using a Langmuir probe (LP) and an emissive probe (EP) were compared. In the ORNL CAPRICE electron cyclotron resonance (ECR) ion source, we show that, for normal ECR ion source operating conditions, the large population of hot electrons may cause the emissive floating point method to fail and may cause the values deduced using the LP method to be uncertain by more than 30 %. Having in this manner determined the magnitude of the possible uncertainties of the deduced potentials, we studied the chamber surface condition effect and the gas mixing effect by comparing in-situ probe measurements with measurements of the extracted ion beam charge state distribution (CSD). The plasma potential values are found to be extremely sensitive to the surface condition of the source chamber walls; a contaminated surface gave plasma potential values that were larger by 10 V. Also, the plasma potential was found to be significantly decreased during gas mixing; the corresponding increase in ion confinement time may be the dominant mechanism responsible for the gas mixing effect.

PACS numbers: 52.50.Dg, 52.70.Ds, 52.75.-d
Keywords: ECR, ECR ion source, Plasma potential, Carbon contamination, Gas mixing, Probe diagnostics

I. INTRODUCTION

It has been well known since Geller's remarks [1] that the plasma potential might be a good indicator for the source performance, specially for improving highly charged ion output from electron cyclotron resonance (ECR) ion source, because many empirical techniques, like wall coatings, secondary electron materials, electron injection and biased disks, and gas mixing, may lower the plasma potential [2]. In this sense, plasma potential measurement and monitoring is very important in understanding the detailed mechanism of the techniques mentioned above and in checking the source performance. In this paper, plasma potential measurements are performed using electrical probes. The motivation for these attempts was a real-time, in-situ, independent determination of the local plasma potential. In the past, other measurements have been done either by using the magnetic analyzer method [2] or by using the decelleration method [3]. However, compared with the probe method, both those methods use the ion beam extracted from the plasma to give the global plasma potential, which is due to their assumption that there is a uniform potential between the plasma and the chamber wall. Therefore, in both those methods, the plasma potential gradient of the internal plasma is not considered; correspondingly, the question of where ions come from should be answered. Even for the magnet analyzer method, apart from the ion optical uncertainty, several measurements with different source voltages have to be done to complete one measurement of the plasma potential. In this sense, the above methods do not easily give an in-situ, real-time, independent determination of plasma potential.

Recently Langmuir probe (LP) diagnostics have been attempted for the first time in ECR ion source [4]. In an ideal (*i.e.*, unmagnetized, collisionless, stationary, and purely Maxwellian) plasma, LP data can be easily analyzed to provide precise values of the plasma potential (V_s). However, due to the geometrically complex, magnetized, and non-Maxwellian nature of ECR plasmas and the large population of fast electrons, determination of V_s from LP data can be problematic [5] and should be confirmed using another diagnostic, such as an emissive probe (EP) or laser-induced fluorescence (LIF) method [6]. In this paper, LP plasma potential determinations were experimentally checked by using an EP. Having determined the magnitude of the possible uncertainties of the deduced potentials, we studied the effects of chamber surface contamination and of gas mixing [7] by com-

*E-mail: hjyou@hanyang.ac.kr; Fax: +82-2-2299-1908

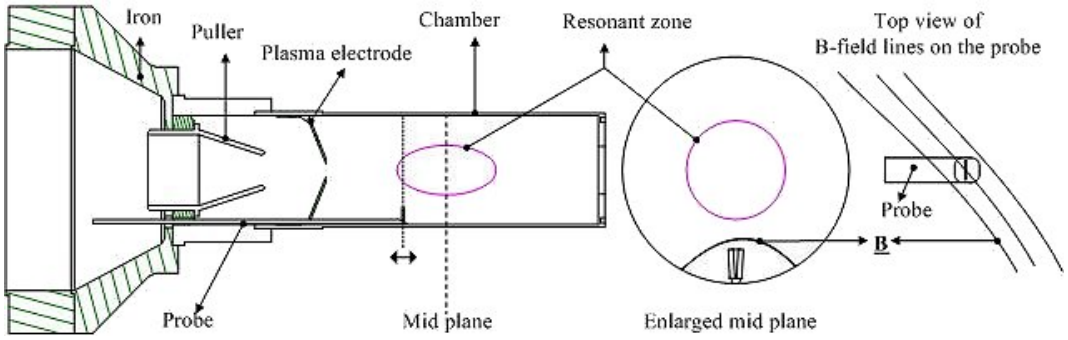

Fig. 1. Probe positioning relative to the radial loss cones of the magnetic structure of CAPRICE ECRIS.

paring probe data with the charge state distributions (CSD's) extracted from the beam.

II. EXPERIMENTS

The experiments were performed with an argon plasma in the ORNL CAPRICE ECR ion source [8, 9], which has a minimum-B structure with a peak axial mirror field of 1.2 T and maximum radial confinement field of 0.9 T at the chamber wall. The argon plasma was created by launching a 10.6-GHz (equal to the cyclotron frequency) of wave of 0.37 T, providing an ellipsoidally shaped resonant surface with axial and radial axes of 5.5 and 3.0 cm, respectively. The stainless steel plasma chamber measures 16.5 cm from the plasma electrode to the end of the coaxial wave launcher and has a diameter of 6.6 cm. Ion beams are extracted at a source potential of 10 kV and analyzed by using a stigmatic magnetic analyzer.

If an electrical probe is to be operate successfully, the probe must be small in comparison to the plasma length so as not to perturb the global state of the plasma and at the same time, be able to withstand the heat load from the plasma without damage. In the case of an ECR plasma, it is difficult to satisfy both requirements simultaneously because of the small plasma length scale and the high heat flux from its large population of hot electrons. In the present measurements, both requirements were satisfied by judiciously placing the probe holder into the edge region of the ECR plasma and by limiting the injected microwave power to values sufficiently low to avoid self-emission of the probe. The probe was inserted in a location where the flux tube intercepted by the probe had no direct connection either to the ECR zone where the electrons are heated or to the extraction region where high-energy backstreaming electrons may be present (see Fig. 1). During the present measurements, careful shielding of the probe leads in the extraction vacuum chamber assured that operation of the in-situ probe when the source was operated at high voltages resulted in no detectable perturbation of the extracted beam currents. The probe could be operated in both the Langmuir probe (LP) and the emissive probe (EP) modes and was formed from $r_p = 0.058$ mm tungsten wire, which extended toward the source axis from two small alumina tubes, forming a small loop of approximately 3 mm length. The electron and ion Larmor radii (r_e, r_i) at the probe positions were estimated to be of the order of 0.01 mm and 0.5 mm, respectively. Consequently, the electrons are magnetized while the ions are unmagnetized. Further, due to the large sheath thickness (s) arising from the low plasma density and the high electron temperature, the probe operates in the collisionless regime for both electrons and ions.

ECR ion source operation at high voltages from 5 to 30 kV presents another technical challenge in operating electrical probes. In the present measurements, the probe electronics (bipolar operational amplifier, oscilloscope...) were floated at the ion source potential, requiring HV isolation between the measuring devices and the data acquisition and control PC. In this experiment, wireless Ethernet connections were first employed for the isolation. Fig. 2 shows a schematic diagram of the probe operation on the CAPRICE ECR ion source using the wireless connection. As Fig. 2 show, both the Labjack UE9 multifunction data acquisition and control device and the TDS3034B oscilloscope were controlled by a laptop computer through the wireless connection: the USB/Ethernet-based Labjack UE9, was used to provide the probe current power supply (P/S) with analog input signals (DAC1) and the HP function generator with digital signals (FIO0) while the TDS3034B oscilloscope was used to measure the probe bias and current signals (V and I). Each device had an Ethernet 10Base-T compatible wireless interface and was linked to an appropriate Ethernet bridge or wireless LAN card. The filament heating P/S could be controlled by using an analog signal (0 to 5V) provided by the Labjack UE9. An AD210 isolation amplifier was used to isolate the filament heating P/S from the Labjack UE9 analog signal. Digital signals from the Labjack UE9 were used to trigger the function generator sawtooth signal output, which was then fed into a Kepco BOP 100-1M amplifier for sweeping the probe bias. The digital signal went to the oscilloscope and simultaneously triggered it. An additional AD210

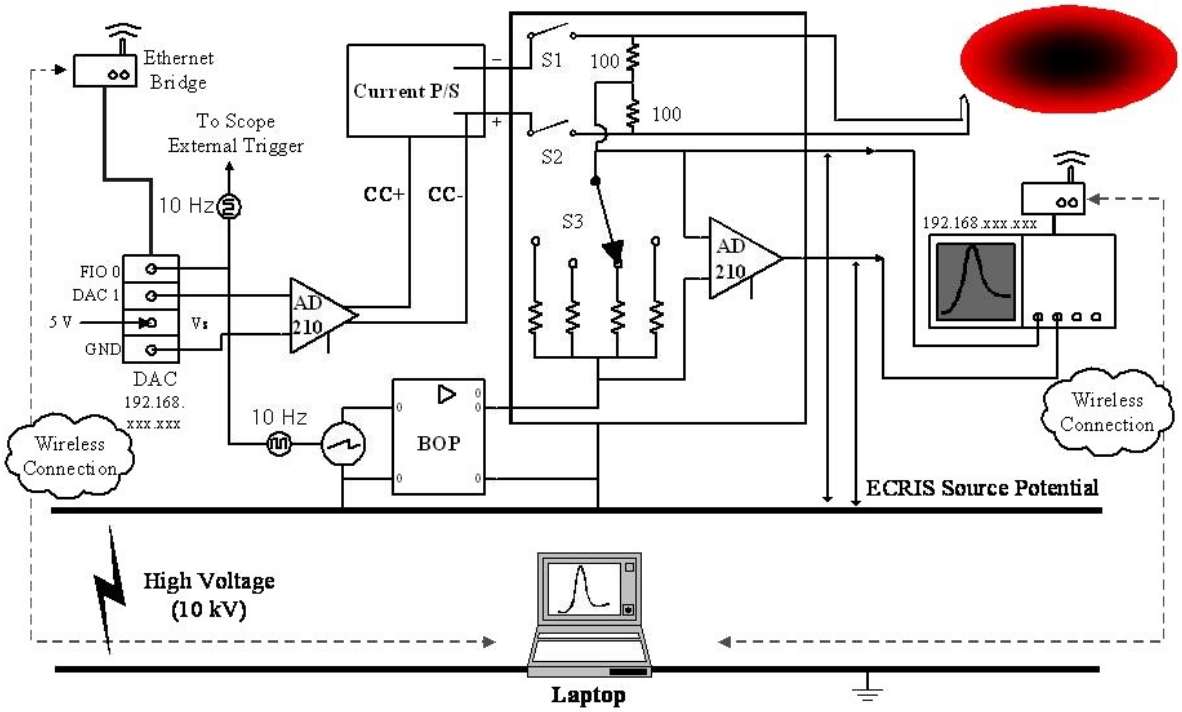

Fig. 2. Probe circuits and their isolated operations via a wireless connection on the ORNL CAPRICE ECR ion source.

isolation amplifier was used to measure the voltage drop across the measuring resistor, as in conventional probe circuits. Two additional switches (S1, S2) were installed to permit changing the probe operation modes between the LP and the EP mode.

All control and data acquisition functions were interfaced using a virtual Labview instrument installed on a laptop computer. Because all control and analysis processes could be completed within a second, the data could be simultaneously acquired, processed, and analyzed in real time. The acquired data were first digitally processed through the use of a modified Savitzky-Golay smoothing filter [10]. The smoothing method was able to provide a smoothed first derivative of the probe I-V characteristic. The voltage at which the maximum of the derivative curve occurred was taken as the plasma potential. This maximum was directly related to the apparatus function of the experiment and to the number of points used for the smoothing [11]. The resolution of the measurement, R_m, could be estimated from the product of the number of smoothing points, n, and the voltage range of the sweep, dV, divided by the point resolution of the measurement, N: $R_m = ndV/N$. During the measurement, R_m was minimized by adjusting the sweep voltage range and the number of smoothing points and then maintained so that its value would make the value always be less than $\frac{3}{2}T_e$, an accepted standard for assuring a reasonable accuracy for the deduced electron distribution [12].

III. RESULTS AND ANALYSES

The plasma potential determined from the LP data is usually taken in the ideal case to be the maximum value of the first derivative $I'(V_P)$) of the probe current with respect to the probe bias (V_p) [10,11,13]. In reality, the plasma state, the probe analysis operating regime, and a range of other effects can result in deviations from this ideal case. The most reliable value, in principle, is found by fitting the data to an appropriate theoretical model [5]. However, such an approach is not amenable to real-time measurements. In the present measurements, because real-time monitoring of the plasma potential were a central focus and because relative changes, not absolute values, in the plasma potential were of interest, the peak value of $I'(V_P)$ was assumed to give the plasma potential.

In order to delineate better the conditions under which the above assumption holds and the magnitude of the error that results when it fails, performed measurements were with the probe operating in the EP mode at two discharge conditions: (a) one is a source pressure of 4×10^{-7} Torr and a microwave power level of 28 W, (b) the other is a a source pressure of 2×10^{-7} Torr and a microwave power level of 36 W, which are all conditions favorable for the generation of highly charged ions and, thus hot electrons. The results are shown in Figs. 3(a) and (b), each of which displays both $I(V_p)$ and $I'(V_p)$ curves at different filament heating currents. The plasma potential was determined by monitoring the $I'(V_p)$ max-

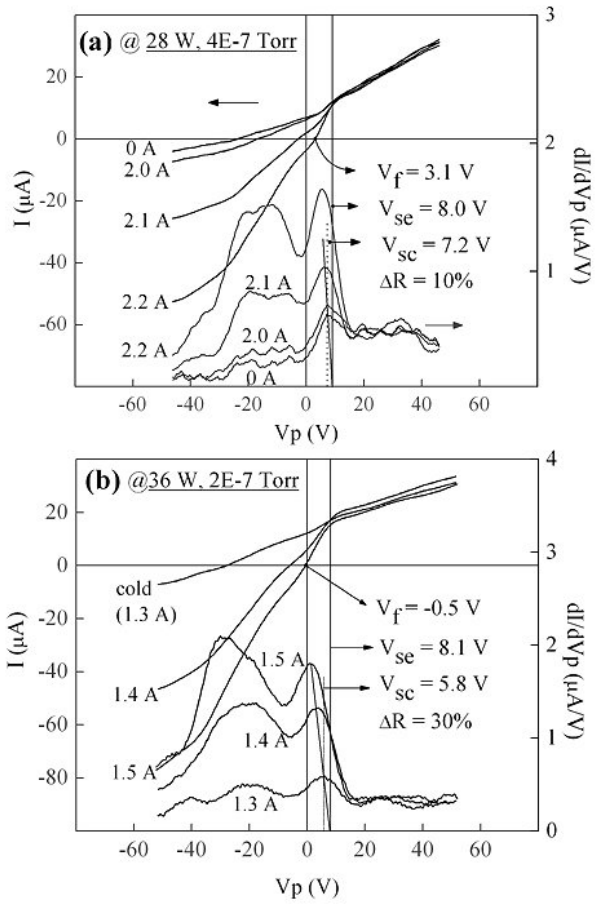

Fig. 3. Plasma potential measurements by an EP at two discharge conditions,(a) a source pressure of 4 × 10^{-7} Torr and a microwave power level of 28 W, and (b) a source pressure of 2 × 10^{-7} Torr and a microwave power level of 36 W, with the same axial field coil currents of 952/1010 A on the injection/extraction sides.

imum as a function of heating current and extrapolating the result to zero electron emission, as illustrated by the solid lines in the figures. These values, denoted by V_{se}, are expected to be the most accurate [14,15]. From the figures two observations are noted. First, the floating potential, V_f, is significantly different from V_{se} even under maximum achievable electron emission conditions: Figs. 3(a) and (b) show the differences between V_{se} and V_f of 4.1 V and 8.6 V, respectively. Second, the $I'(V_p)$ maxima in the LP mode, denoted by V_{sc} and the dotted line in the figures, differ from V_{se} in these cases by 10 % for condition (a) and 30 % for condition (b). For other plasma conditions, differences of more than 30 % were observed. These features suggest that for typical ECR source conditions, the presence of fast electrons can lead to erroneous plasma potential values in both the emissive floating potential method and in the LP approach.

Usually surface contamination of the plasma chamber deteriorates the production of high-charge ions [16]. This is why the plasma chamber should be periodically cleaned. In order to study the surface contamination effect, we performed the plasma potential measurements using the LP and the EP methods for plasmas with three different surface condition of the plasma chamber: (1) a carbon contaminated chamber, (2) a chamber partially cleaned by Ar-plasma-stimulated desorption, and (3) a chamber cleaned by using a bead blaster. For surface condition (1) the plasma chamber was contaminated partly by carbon products (during 1 week's CH4 plasma operation) and partly by water-vapor adsorption (during 20 minutes' venting for probe installation). Condition (2) is accomplished by a 5 hours' high-pressure (10^{-6} Torr) operation with an Ar plasma. For condition (3) a spherical glass bead blaster was used to minimize bulk material removal and to give a "peening-like" surface conditioning effect. The blaster method is known to be effective in removing the carbon layer deposited on the chamber. Measurements were attempted to correlate the plasma potentials with external CSD's. The external CSD's for the three surface conditions are displayed in Figs. 4 (a), 4(b), and 4(c), and the measured plasma potentials are shown in Fig. 4(d). It is noted that all of the CSD's in Fig. 4 are results optimized for getting a maximum Ar^{8+} beam with the same rf power level and magnetic field configuration. The Ar gas flow rate was the only control factor for the optimizations. As can be seen in Fig. 4(a), there are many impurities (oxygen, carbon, nitrogen, and hydrogen); the impurities' ion beams are much higher than the intended Ar beams; for the Ar beams, it appears that there is very small level of low charge state ions, indicating indicating that the impurities from the chamber wall should increase the neutral pressure inside the ECR plasma and might limit the production of the Ar beam. In Fig. 4(b), the oxygen and the carbon beams are substantially decreased, but still exist at a low level, while the Ar-ion beams are increased by a factor of 5 for low-charge ions(Ar^{2+} to Ar^{4+}), and by a factor of 2 for medium-charge ions (Ar^{6+} to Ar^{7+}), but they are on the same level for high-charge ions (Ar^{8+}, Ar^{9+}). Comparing the CSD's in Figs. 4(a) and 4(b), even though the total Ar beam current of surface condition (1) is lower than that of condition (2), the beam current ratio of the high-charge ions to the low-charge state ions in Fig. 4(a) are much higher than that in the CSD of Fig. 4(b). Oxygen gases from the wall are expected to greatly help the generation of high-charge ions: oxygen is known to be the best mixing gas for highly-charged-ion production.

It is noted that the plasma potential was not changed much in the above two cases, still being around 20 V. However, the plasma potential was substantially decreased by 10 V for condition (3). Fig. 4(c) for the corresponding CSD of condition (3), shows that high-charge ions (Ar^{8+}, Ar^{9+}) are doubly increased and that the impurities are decreased to low levels. From the the larger change of plasma potential, the different CSD's shown in Figs. 4(b) and 4(c) should mostly come from a decrease in the plasma potential caused by the differ-

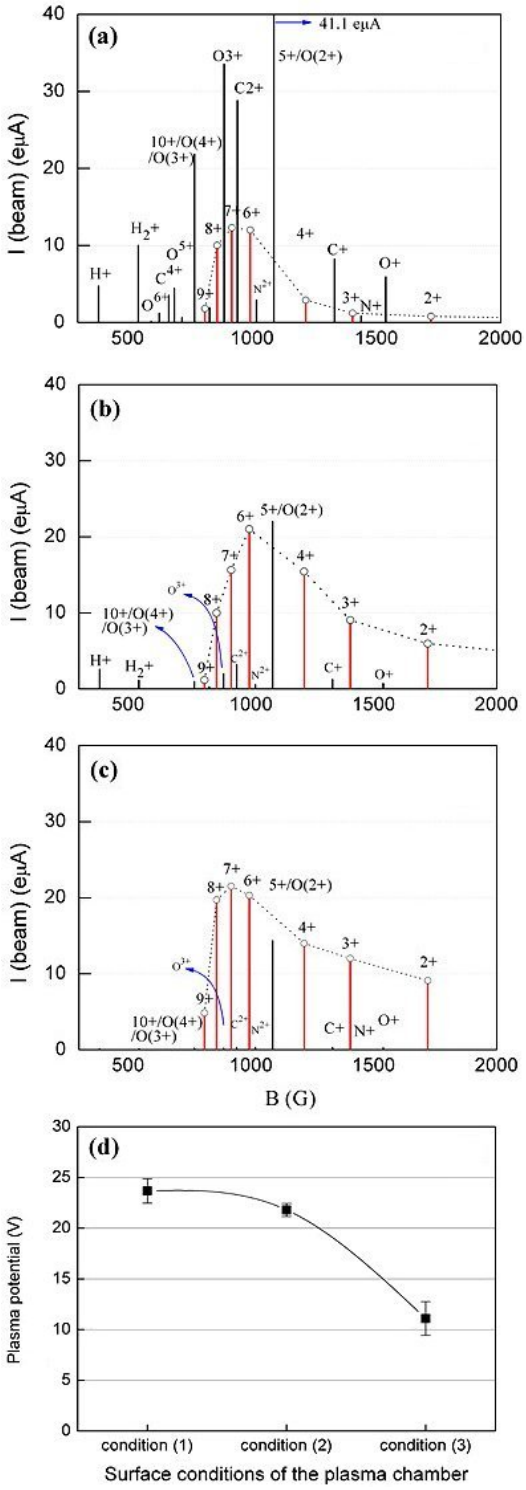

Fig. 4. External beam charge state distributions (CSD's) and the measured plasma potentials for three different surface conditions of the plasma chamber, (a) a carbon-contaminated surface, (b) a surface partially cleaned by using an Ar plasma for 5 hours, (c) a surface cleaned by using a glass bead blaster, and (d) the measured plasma potentials for the three surface conditions.

ence in the surface conditions: the carbon layer seems to be almost completely cleared in the case of condition (3) when comparing the impurity levels in Figs. 4(b) and 4(c).

At this point, one may questioned what makes the plasma potentials different. This could be answered from the change in the secondary electron coefficient of the chamber wall: Carbon coated stainless steel has been reported to give a average secondary electron coefficient of 0.88 for normal incidence - a reduction of almost 40 % compared to untreated stainless steel [17]. According to plasma-boundary physics, wall surfaces that emit cold electrons into a plasma reduce the sheath potential drop, thus reducing sputtering significantly [18]. Explaining this qualitatively, the plasma potential adjusts itself to have a quasi-neutrality condition under the condition of secondary electron emission from the wall; a larger electron emission from the cleaned wall causes plasma potential to be smaller if the ion and electron loss are be the same. Correspondingly, the loss of ions to the wall is reduced due to the lowered plasma potential, and the lowered sputtering by highly charged ions will help the plasma to become more stable.

Some gas mixing effect studies were carried out, as well. The measurements used the LP method to obtain both the plasma potential, V_s, and the fast electron temperature, T_{ef}, and were focused on the correlation of these plasma parameters with external Ar CSD's modified by the addition of helium and oxygen mix gases. Four different Ar plasmas were investigated: a pure Ar plasma, an Ar/He plasma, and two Ar/O_2 mixtures. In the first Ar/O_2 mixture and the Ar/He mixture, the Ar leak rate was kept at the rate determined for the pure Ar case to give a maximum Ar^{8+} current while the mix-gas flow rate was adjusted to further optimize the Ar^{8+} current. For the second Ar/O_2 mixture, both gas flow rates were optimized for maximum Ar^{9+} current. For all 4 mixtures, slight adjustments of the rf power and the axial magnetic field strength were also made. After each optimization, a number of LP measurements were made and recorded. The experimental parameters for each mixture are summarized in Table 1, and the corresponding CSD's are shown in Fig. 5(c). The LP $I'(V_p)$ curves are shown in Fig. 5(a), and the peak positions, assumed to correspond to the relative plasma potential, are summarized in the final column of the Table 1. Prior to these measurements, the plasma potential's dependence on the power, pressure, and axial magnetic field was more extensively mapped in a pure Ar plasma. Typical trends found were that the plasma potential increases by less than 5 V as the source pressure went from 2×10^{-7} to 10×10^{-7} Torr and as the rf power increased from 10 to 50 W, and that there was only a weak dependence on B-field. Therefore, small variations of the pressure, magnetic field, and rf power in the gas mixing measurements should not have contributed significantly to the observed differences in the plasma potential.

In addition to the plasma potential, fast electron tem-

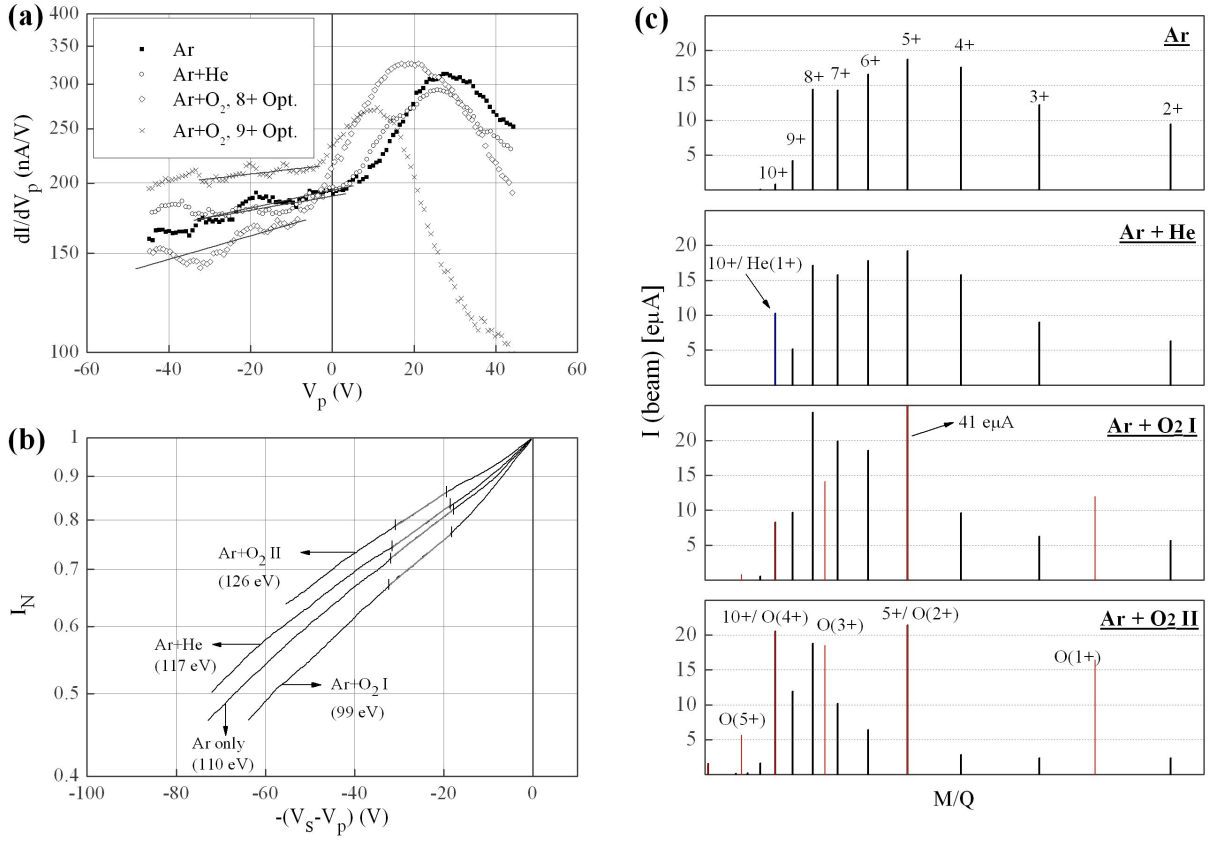

Fig. 5. Langmuir probe measurements of (a) plasma potentials and (b) fast electron temperatures; (c) corresponding external beam charge distributions (CSD's) for pure Ar, Ar+He and Ar+O_2 plasmas.

Table 1. Experimental conditions for the gas mixing studies.

	rf power (W)	Source Pressure (× 10^-7)(Torr)	V_s (V)
Ar	30	1.8	27 ± 0.4
Ar+He	30	2.0	23 ± 1.2
Ar+O_2 I	31	20.0	18 ± 1.5
Ar+O_2 II	34	12.0	10 ± 0.5

peratures (T_{ef}) were obtained from the LP data. Fig. 5(b) shows I-V curves (I_N) drawn on a semi-logarithmic scale, normalized by dividing by the electron saturation current taken at the maximum of $I'(V_p)$. T_{ef} can be extracted from the curves by fitting only the linear part of the normalization curve (see values in parentheses in Fig. 5(b)). This direct fitting of $\ln(I_N)$ is possible only when the fast electron contribution dominates and when temperature of the hot electrons is sufficiently different from that of the cold electrons. The present plasma conditions satisfy both conditions. Based on other investigations in magnetized plasmas, this fitting approach can overestimate the fast electron temperature by up to 30 % [5]. It is noted that, unlike the plasma potential, T_{ef} was found to be very sensitive to small changes in the plasma conditions, particularly the rf power level. It is known from probe theory [19,20] that in magnetized plasmas, the electron energy distribution (EEDF) is proportional to I'(Vp). The long tails extending to the left of the $I'(V_p)$ peaks in Fig. 5(a), therefore, provide further evidence for the presence of significant populations of fast electrons, which are obviously closely related to the generation of the highly charged ions observed in the extracted CSD's. Both variations in the plasma potential and in fast electron temperature with gas mixing show a correlation with the changes in the CSD's shown in Fig. 5 (c). The observed 30 % variation in T_{ef} is ascribed mainly to varying source conditions. From the much larger change (factor of 2.7) of the plasma potential found in going from the pure Ar to the Ar+O_2 II case, the earlier noted lack of sensitivity of Vs to source conditions, and the greatly different CSD's for these two cases, it would appear that a decrease in the plasma potential and a corresponding increase in the ion con-

finement time is the dominant mechanisms responsible for the gas mixing effect. Similar conclusions have been reached by other groups [2, 21]. Lastly, it is important to note that when closing the He gas valve, the plasma parameters and the CSD immediately returned to their original values (pure Ar case) while a much longer time interval (about a half hour) was required after closing the O_2 mix gas, suggesting significant surface sticking for this gas. To our knowledge, this was recognized for the first time in this plasma potential experiment. As we observed above for oxygen gas mixing, there appears to be an additional effect of oxygen's surface conditioning, apart from the ion cooling effect that has been regarded as the most plausible explanation for the gas mixing effect [7].

IV. CONCLUSIONS

Real-time and in-situ plasma potential measurements by use of a Langmuir probe and an emissive probe were successfully performed in the edge plasma of the ORNL CAPRICE ECR ion source. The plasma potential values deduced using the LP method are shown to have in uncertainties by more than 30 %, which are very dependent on the presence of hot electrons; also a large population of hot electrons was shown to cause the emissive floating point method to fail. Based on the determined possible uncertainties and proper positioning of the probe, the chamber contamination effect and the gas mixing effects were studied by comparing the measured plasma potential with the measurements of the extracted ion beam CSD. The plasma potential values was found to be extremely sensitive to the chamber surface conditions; a contaminated surface gave a plasma potential values larger by a factor of 2. Also, the plasma potential decreased with gas mixing. In addition, it is worth noting that oxygen gas mixing gave a much lower plasma potential, suggesting significant surface sticking and causing the modification of the chamber surface's condition.

ACKNOWLEDGMENTS

H. J. You acknowledges support from the International Research Internship Program and the National Research Laboratory Program of the Korea Science and Engineering Foundation (KOSEF) under the Ministry of Science and Technology (MOST) of Korea with additional support from Office of Basic Energy Sciences and Office of Fusion Energy Sciences of the U.S. Department of Energy under contract DE-AC05-00OR22725 with UT-Battelle, LLC.

REFERENCES

[1] R. Geller, *Electron Cyclotron Resonance Ion Sources and ECR Plasmas* (IOP, Bristol, 1996), p. 267.
[2] Z. Q. Xie and C. M. Lyneis, Rev. Sci. Instrum. **65**, 2947 (1994).
[3] O. Tarvainen, P. Suominen and H. Koivisto, Rev. Sci. Instrm. **75**, 3138 (2004).
[4] L. Kenéz, S. Biri, J. Karácsony and A. Valek, Nucl. Inst. Meth. B **187**, 249 (2002).
[5] V. I. Demidov, S. V. Ratynskaia and K. Rypdal, Rev. Sci. Instrum. **73**, 3409 (2002) and references therein.
[6] H. J. Woo, K. S. Chung, T. Lho and R. McWilliams, J. Korean Phys. Soc. **48**, 260 (2006); G. D. Severn, Xu Wang, E. Ko and N. Hershkowitz, Phys. Rev. Lett. **90**, 145001-1 (2003).
[7] A. G. Drentje, Rev. Sci. Instrum. **63**, 2875 (1992).
[8] B. Jacquot and M. Pontonnier, Nucl. Instrum. Meth. Phys. Res. A **287**, 341 (1990).
[9] F. W. Meyer, *Trapping of Highly Charged Ions: Fundamentals and Applications*, edited by J. Gillaspy (Nova Science, New York, 2000), p. 117.
[10] F. Fujita and H. Yamazaki, Jap. J. Appl. Phys. **29**, 2139 (1990).
[11] J. I. F. Palop, J. Ballesteros, V. Colomer and M. A. Ernandez, Rev. Sci. Insrum. **66**, 4625 (1995).
[12] V. A. Godyak, R. B. Piejak and B. M. Alexandrovich J. Appl. Phys. **73**, 3657 (1993).
[13] D. N. Ruzic, *Electric Probes for Low Temperature Plasma*, edited by Wood Weed (The American Vacuum Society Education Committee, New York, 1994), p. 46.
[14] N. Hershkowitz, IEEE Trans. Plasma Sci. **22**, 11 (1994).
[15] J. R. Smith, H. Hershkowitz and P. Coakley, Rev. Sci. Instrum. **50**, 210 (1979).
[16] O. Tarvainen, P. Suominen, H. Koivisto and I. Pitkanen, Rev. Sci. Instrum. **75**, 1523 (2004).
[17] D. Ruzic, R. Moore, D. Manos and S. Cohen, J. Vac. Sci. Technol. **20**, 1313 (1982).
[18] L. A. Schwager, W. L. Hsu and D. M. Tung, Phys. Fluids B **5**, 621 (1993).
[19] V. I. Demidov, S. V. Ratynskaia, R. J. Armstrong and K. Rypdal, Plasma Sources Sci. Technol. **6**, 350 (1999).
[20] R. R. Arslanbekov, N. A. Khromov and A. A. Kudryavtsev, Plasma Sources Sci. Technol. **3**, 528 (1994).
[21] Y. Kato, M. Saitoh, Y. Kubo and S. Ishii, *IEEE Proceedings of the 11th Int. Conf. on Ion Implant. Technol.* Vol. 1 (Texas, 1996), p. 418.